

Diagnosics Specificity of Variable Vertical Axis Rotor With Damaged Bearings

A. Tadžijėvas¹
 Klaipėda University
 Klaipėda, Lithuania

V. Barzdaitis²
 Kaunas University of Technology
 Kaunas, Lithuania

R. Didžiokas³
 Klaipėda University
 Klaipėda, Lithuania

V. Ostasevičius⁴
 Kaunas University of Technology
 Kaunas, Lithuania

Abstract. This article presents theoretical and experimental research results of a variable axis vertical rotor with imbalance and artificially damaged deep groove ball bearings 6004-2Z/C3. The rotor imbalance has been varied from low level, permissible value according ISO 1940 and high value in order to determine how the magnitude of imbalance contributes to the bearing's outer ring raceway spalls masking defect. The general dynamic force acting in variable vertical rotational axis rotors composed of rotor mass gravity force and unbalance generated force. In order to increase rotor's defects diagnostic procedure accuracy and identification of technical condition of antifriction bearings absolute housings vibration measurement data transformed to the designed statistical parameter DVR (Defect Visibility Ratio).

Keywords: variable axis vertical rotor, bearing outer ring raceway spall, diagnostics, vibration, dynamic force, Defect Visibility Ratio

I. Introduction

The one of the major defect diagnostics problems of variable vertical axis rotors with antifriction bearings are the identification of imbalance generated force acting together with rotors mass gravity force, and described as general dynamic force F_s , and bearings outer rings raceways spall. This article has link with author's previous research results concerning vertical and horizontal rotational axis rotors with damaged antifriction bearings elements defect diagnostics as described in articles [1, 2]. The vertical axis rotating machines with antifriction bearings are widely spread in industry as various types of centrifuges, pumps, fans, marine ships machines, etc. The imbalances of vertical rotors are one of main factors that cause failures of bearings elements. The research results of vertical rotors dynamics mostly eliminates gravity force acting in radial-orthogonal directions of bearing housing's [3]. There are many research articles, concerning horizontal axis rotors dynamics and defects diagnostics when rotors have imbalance, misalignment and bearings elements kinematics defects [4, 5, 8 - 10]. The vertical rotors misalignments is less problem in comparison with horizontal axis rotors, because vertical rotors design schemes usually have integrated housings. The more actual problem of vibration severity evaluation and failures diagnostics of vertical rotors concerns technical-technological-thermal imbalances together with bearings elements defects as spalls in raceways. The theoretical and experimental study of dynamics of variable vertical axis rotors with imbalances and damaged bearings

outer rings raceways has the task to design more efficient defect diagnostic's method for practical usage of vertical rotors condition monitoring and diagnostics. This task was achieved through investigation of forces acting on vertical rotors bearings housings, when vertical rotational rotor's tilting axis position varies and bearings outer rings raceways artificial defects included.

II. Dynamic Force of Vertical Axis Rotor

There is some difference in modeling idea between horizontal and vertical axis rotors. It was accepted that two acting forces exist in orthogonal planes in vertical axis rotors: eccentric inertia force caused by imbalance u acting perpendicular to rotation axis and second – axial force as gravity force F_{mg} of rotor's mass m acting parallel to vertical axis, Fig.1.

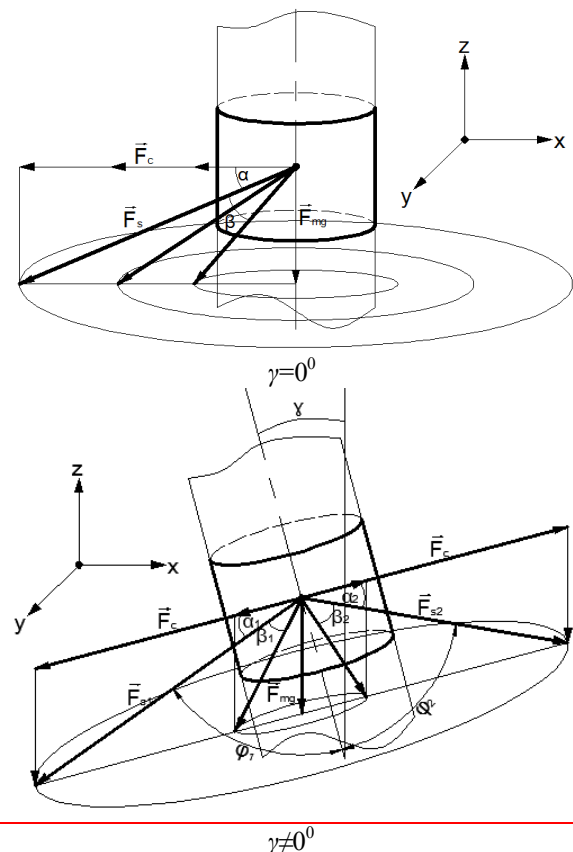


Fig.1 Schemes of the forces acting in the vertical rotating rotors with imbalances $u = m_u r_u$ and varying vertical axis tilting angle $\gamma=0^0$ and $\gamma \neq 0^0$; $F_c = (m_u r_u) \omega^2$ -eccentric unbalance mass m_u inertia force; $F_{mg} = m g$ - rotor's mass m gravity force; $F_s (F_{s1}, F_{s2})$ - dynamic forces position angles ϕ_1 and ϕ_2

¹arturas.tadzijevas@ku.lt
²vytautas.barzdaitis@ktu.lt
³Rimantas.Didziokas@ku.lt
⁴vytautas.ostasevicius@ktu.lt

In horizontal axis rotors eccentric inertia force F_c proportional to imbalance u and gravity force F_{mg} of rotor's mass m acting both perpendicular to rotation axis. The dynamic force F_s in vertical rotors varies in module and in position angle relative to vertical rotation axis. The dynamic force F_s partly loaded bearings in axial direction. The angle α between dynamic force F_s and eccentric inertia force F_c is shown in Fig.1.

F_s -dynamic force is constant during full rotation, when rotor's vertical axis tilting angle $\gamma=0^0$, and calculated according (1).The axial force acting on the bearing equals to gravity force F_{mg} .

$$F_s = \sqrt{F_{mg}^2 + F_c^2}. \quad (1)$$

Dynamic force F_s vector phase angle α reference to unbalance force F_c is changing when imbalance force F_c changes or gravity force is changing:

$$\alpha = \arccos \frac{F_c}{F_s}. \quad (2)$$

When gravity force F_{mg} increases (e.g. in vertical centrifuges), the dynamic force F_s module and phase angle α increases in vertical axis rotors with $\gamma=0^0$, when eccentric inertia force F_c is constant. When eccentric inertia force F_c increases (e.g. technological imbalance increases during machine operation, rotors rotational speed increases) the dynamic force F_s module increases, but phase angle α decreases. The dynamic force F_s position angle φ changes reference to rotational axis. This is the reason that failures diagnostics of vertical rotors using vibration measurement data of the bearing housings are more complicated in comparison with horizontal rotors. This feature is important for varying rotational speed of sugar production centrifuges, for sea ships machines condition monitoring and failures diagnostic, particularly for machines mounted on flexible low stiffness foundations.

In the horizontal axis rotors the dynamic force F_s module varies in radial plane always positioning perpendicular to rotation axis, but the phase angle does not change its value versus horizontal rotor's rotational axis. The F_s force does not generate axial dynamic force in horizontal rotors with imbalance and varies as minimum F_{smin} and maximum F_{smax} dynamic forces:

$$\begin{cases} F_{smin} = F_c - F_{mg}, \\ F_{smax} = -(F_c + F_{mg}). \end{cases} \quad (3)$$

In the sea ships the tilting angles are limited in longitudinal direction $12,5^0-15^0$ and in transverse direction 15^0-20^0 with permissible accelerations in vertical direction up to 1,0 g and in transverse direction up to 0,6 g. The vertical axis machines rotors position reference to ideal vertical rotational axis is defined by tilting angle γ , Fig. 1. When tilting angle $\gamma \neq 0^0$ the variation of dynamic force value ΔF_s is evaluated according (4).

$$\Delta F_s = F_{s1} - F_{s2}, \quad (4)$$

where F_{s1} – maximum and F_{s2} – minimum dynamic forces as presented in Fig.1.

$$F_{s1} = \sqrt{F_c^2 + F_{mg}^2 + 2F_c F_{mg} \sin \gamma},$$

$$F_{s2} = \sqrt{F_c^2 + F_{mg}^2 - 2F_c F_{mg} \sin \gamma}.$$

Rotors vertical axis tilting angle γ describes rotor rotation axis position versus ideal vertical axis position and explains changing module and angle position of dynamic force F_s . The dynamic force synchronizes with rotors rotational speed. This force loads bearings in radial and axial directions, as shown in Fig.1.

The axial force varies and evaluated by value ΔF_{as} (5)

$$\Delta F_{as} = F_{mg} - F_{mg} \cos \gamma. \quad (5)$$

The radial force varies and evaluated by value ΔF_{rs} (6)

$$\Delta F_{rs} = (F_c + F_c \sin \gamma) - (F_c - F_c \sin \gamma) = 2F_c \sin \gamma. \quad (6)$$

These varied axial and radial forces make rotor's and bearings condition monitoring and failure diagnostic procedure complicated. Modeling of vertical axis rotors and simulating forces acting on bearings makes failure diagnostics procedure more adaptive for practical usage.

III. Modeling and simulation of vertical axis rotor

Modeling and simulation of vertical axis rotor provided with FEM and ANSYS software [6, 7]. The designed physical model of vertical rotor is shown in Fig. 2. and model designed with FEM in Fig. 3. The rotor total mass 2.80 kg, shaft length is 0.6 m, diameter 0.02 m, wheel diameter 0.15 m with radius $r_u=0.06$ m for the fixing imbalance masses, two stiffness elements in radial direction of 1st (upper) bearing and three stiffness elements - two in radial direction and one in axial direction - of the 2nd (lower) bearing.

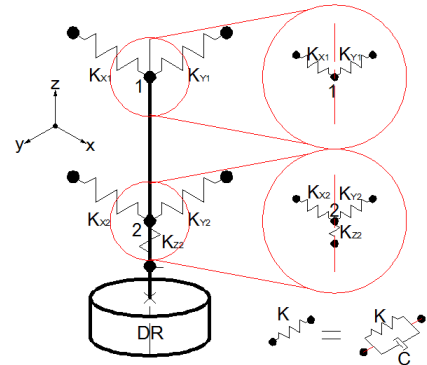


Fig. 2. Physical model of vertical rotor and elements

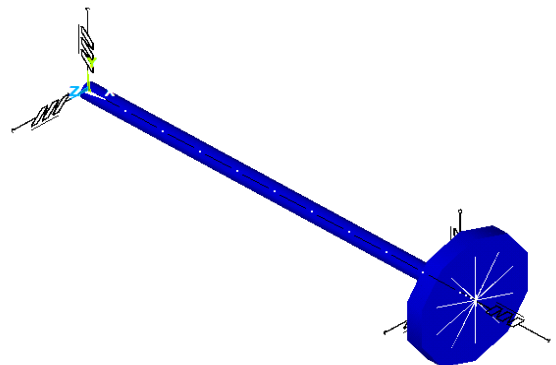


Fig. 3 Vertical rotor FEM model used with software ANSYS simulation

The FEM beam type BEAM188 10 elements used for modeling shaft of the rotor. The beam type BEAM188 3 elements used for the wheel with unbalance mass modeling by element MASS21. For nonlinear bearings stiffness elements the COMBIN39 element and for stiffness-damping linear bearing elements the COMBIN14 element was used.

The bearings nonlinear stiffness elements K_{xi} , K_{yi} and K_{z2} parameters for COMBIN39 elements experimentally measured with testing machine Zwick/Roell Z100 (Germany) in axial and radial directions. Simulations of FEM model were provided in series: with static analysis evaluating constant forces; frequency analysis for determining resonance frequencies; harmonic analysis and transient dynamics analysis axis symmetrical problem and axis asymmetrical problem solving. There were used such mathematical models: Static analysis model $[K]\{u\} = \{F\}$; Modal analysis model $[[K] - \omega^{-2}[M]]\{u\} = 0$; Harmonic response analysis model $[M]\{\ddot{u}\} + ([C] + [C_{gyr}])\{\dot{u}\} + [K]\{u\} = \{F\}$; Transient dynamic analysis model $[M]\{\ddot{u}\} + ([C] + [C_{cor}])\{\dot{u}\} + ([K] - [K_c])\{u\} = \{F\}$ where: $[K]$ – stiffness matrix, $\{u\}$ – nodes displacements vector, $\{F\}$ – acting forces vector, $[M]$ – mass matrix, $[C]$ – damping matrix, $[C_{gyr}]$ – gyroscopic matrix, $\{\omega\}$ – angular velocity vector, $[C_{cor}]$ – Coriolis matrix; $[K_c]$ – spin softening matrix [5]. According to simulation results the dynamic force F_s module and force position angle φ increases nonlinearly with increasing angular velocity ω , imbalance u and rotor's axis tilting angle γ .

The simulation results presented in Fig. 4 and Fig. 5 as vertical axis tilt angle γ influences on dynamics of F_s and position angle φ . The simulation provided when variable vertical axis tilt angle γ values change in discrete steps 5° , 10° , $13,5^\circ$ degrees. The F_s module varies in wide range from 168 N up to 203 N with increasing tilt angle γ , Fig. 4 and exaggerated with increasing rotor's unbalance.

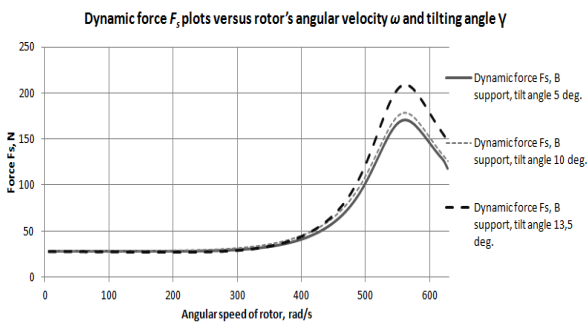


Fig. 4. The 2nd bearing's dynamic forces $F_s(\omega, \gamma)$ plots versus rotor's angular velocity ω and tilt angle γ (5° , 10° and 15°) with imbalance $u_{per}=120$ g mm

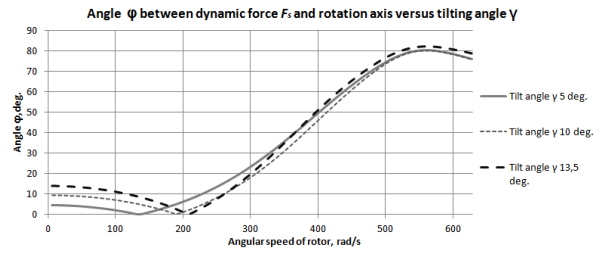
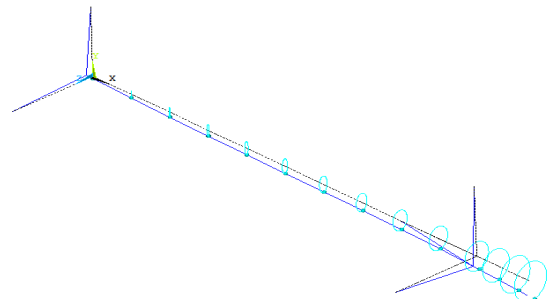
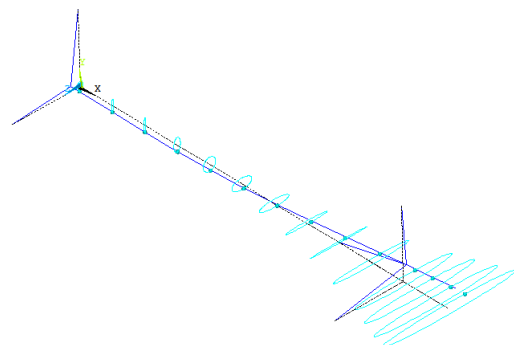


Fig. 5 The 2nd bearing's dynamic forces F_s position angles $\varphi(\omega, \gamma)$ plots versus angular velocity ω and tilt angle γ (5° , 10° and 15°) with imbalance $u_{per}=120$ g mm

It happens that up to first resonance frequency $\omega_R=204$ 1/s the dynamic force F_s position angle φ decreases and becomes $\varphi=0^\circ$ value, Fig. 5 and Fig. 6. Further increasing the angular velocity from $\omega_R=204$ 1/s, the F_s position angle φ increases nonlinearly. For example, when $\omega=314$ 1/s, imbalance $u_L=80,4$ g mm the simulated position angle $\varphi=22^\circ$ and when angular velocity is high $\omega=559$ 1/s imbalance $u_L=80,4$ g mm the position angle increased up to $\varphi=77^\circ$. At resonance rotational angular velocity $\omega_R=204$ 1/s kinetic orbit drastically changes in magnitude and phase angle in comparison with $\omega_L=100$ 1/s and $\omega_H=314$ 1/s angular velocities, Fig.6. These results indicated that failures diagnostics indications of vertical axis rotors are too different in comparison with the horizontal axis rotors.



$\omega_L=100$ 1/s



$\omega_R=204$ 1/s (resonance angular velocity)

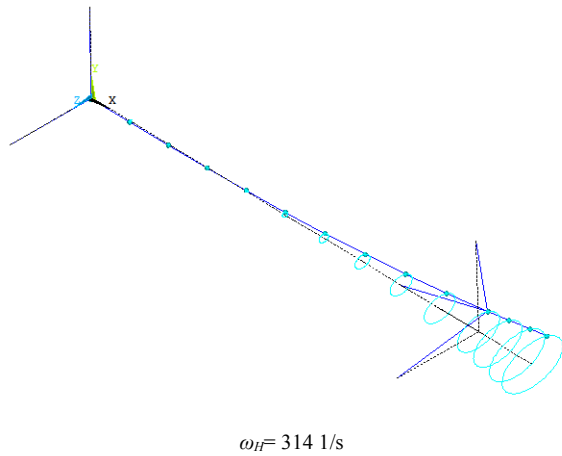
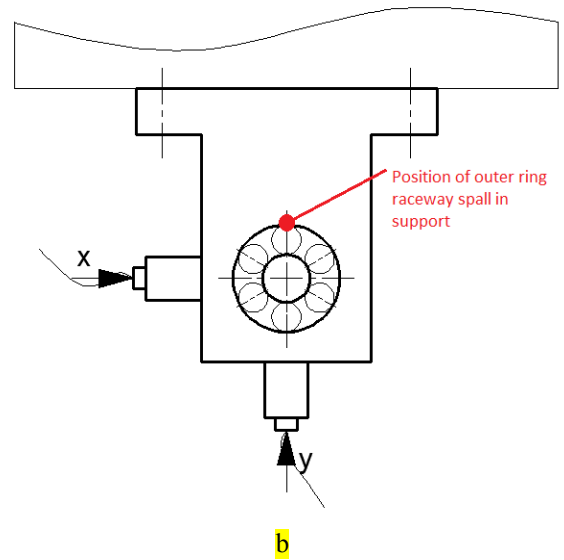


Fig. 6. The vertical axis rotor wheel center kintic orbits when tilt angle $\gamma=13,5^\circ$, wheel unbalance $u_u=80,4$ g mm and different angular velocities: ω_L - low, ω_R - resonance and ω_H - high values



IV. Research kit and experimental results

The experimental test rig in Fig. 7 comprises of rigid frame on which the rotor system is mounted. The system powered with 370 W asynchronous electric motor with current frequency inverter (SSD Drives, model 650V/003/230F) control, elastic coupling, 20 mm diameter and 600 mm length shaft, two bearing's housings with SKF 6004-2Z/C3 deep groove ball bearings 1, 2 and flywheel disc with holes for imbalance masses fixation at radius $r_u=60$ mm. The artificially damaged 2nd bearing outer raceways fixed in the housing.

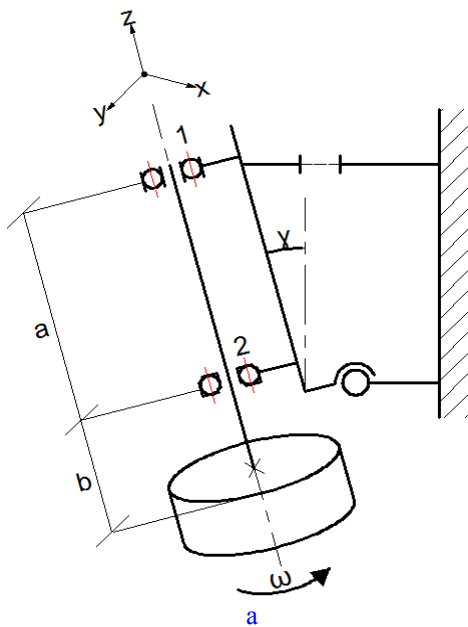
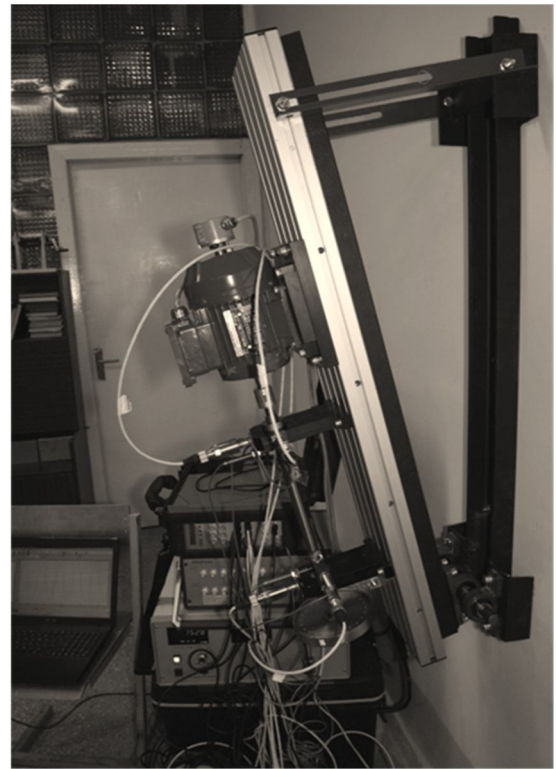


Fig. 7. Vertical axis rotor kit scheme (a) with variable tilt angle γ , piezoelectric transducers X, Y locations at 1st and 2nd bearings housings and position of outer ring raceway spall (b); photo of the research kit (c); bearing outer ring spall 3 mm diameter (d)

Each tested bearing 6004 2Z/C3 has artificially manufactured outer ring raceway spalls: 1,4 mm and 3,00 mm diameter, Fig. 7. The bearings outer ring raceway spall in the bearing's housing located in the Y transducer attached position as shown in Fig. 7. The experiment has been carried out with increasing rotor's rotational speed up to 3000 r/min, constant running at 3000 r/min and decreasing to stand stop. The 6004 2Z/C3 bearing's with outer ring raceway one spall bearing's ball pass frequency (BPFO) theoretically calculated at nominal rotational speed 3000 rpm is $f_{BPFO} = 168,4 \text{ Hz}$. Rotor's imbalance was changed from low value $u_L = 90 \text{ g mm}$ ($m_{uL} = 1,5 \text{ g}$), permissible value $u_{per} = 120 \text{ g mm}$ ($m_{u_{per}} = 2,0 \text{ g}$) for G6,3 balancing quality Grade (ISO 1940-1) and high value $u_H = 156 \text{ g mm}$ ($m_{uH} = 2,56 \text{ g}$). The imbalances were variable in order to determine how the magnitude of imbalance contributes to the bearing's outer raceway failures masking effect. Angular position of vertical axis rotor was changed as tilt angle varies in wide range $\gamma = 0^0 \dots 13,5^0$. Vibration of bearing's housings measured with the Wilcoxon Research transducers model 793, sensitivity 100 mV/g (USA) and processed with signal analyzer OROS Mobi-Pack OR-36 (FR), software OROS NVGate V7.00 and OROS ORBIGate V3.00 (FR) and oscilloscope Scopi XII OX7104 (Metrix, FR).

The 2nd bearing vibration velocity (measured with 2Y transducer) spectrum in vibration velocity cascade format is presented in Fig. 8. The vibration measured with 2X and 2Y transducers and plotted in cascade format has limited information for vibration source identification and defect value evaluation of rotor with imbalance and damaged bearing. The BPFO and harmonics vibration velocity amplitudes are too low and not significant for bearing outer raceway failure evaluation in diagnostics procedure. The unbalance generated vibration velocities amplitudes of 1X frequency synchronized with increasing rotational speed up to $n = 3000 \text{ rpm}$ dominated in the vibration velocity cascade spectrum and damaged bearings BPFO frequency $f_{BPFO} = 168,4 \text{ Hz}$ and harmonics ($nX \text{ def.}$) vibration velocity amplitudes values are too low.

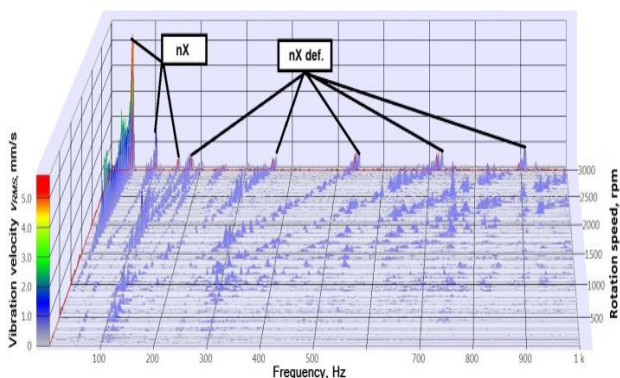


FIG. 8. The 2nd bearing vibration velocity spectrum in cascade format plot during rotor acceleration up to 3000 rpm measured by 2Y transducer; nX-rotor's synchronized rotational speeds frequencies and harmonics; nX-def.-bearings BPFO and harmonics vibration velocity amplitudes; tilt angle $\gamma = 13,5^0$; spall diameter 3,00 mm; permissible imbalance value $u_{per} = 120 \text{ g mm}$

In order to make the procedure of bearings defect diagnostics practically quantifiable and efficient in technical condition evaluation, the statistical parameter "Defect Visibility Ratio" (*DVR*) was designed [1, 2]. The *DVR* is calculated as the vibration parameter velocity of dominant bearing outer raceway defect frequency (BPFO) values v_{RMS_DEF} dividing by rotors synchronous rotation frequency 1X vibration velocity v_{RMS_1X} values (7).

$$DVR = \frac{v_{RMS_DEF}}{v_{RMS_1X}} \quad (7)$$

where: v_{RMS_DEF} – bearing BPFO dominant defect characterized by nX_{def} frequencies harmonics v_{RMS_DEF} values, mm/s; v_{RMS_1X} – rotor synchronous rotation 1X frequency vibration velocities v_{RMS} values, mm/s.

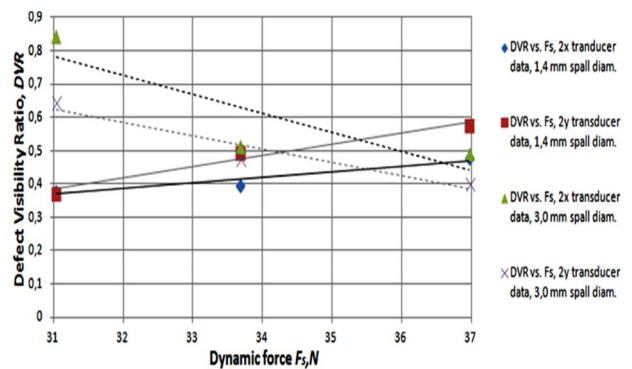


Fig. 9. DVR versus dynamic force F_s plots (imbalances $u_L = 90 \text{ g mm}$, $u_{per} = 120 \text{ g mm}$ and $u_H = 156 \text{ g mm}$): spall diameters 1,4 mm and 3,0 mm, $\gamma = 0^0$, rotational speed $n = 3000 \text{ rpm}$

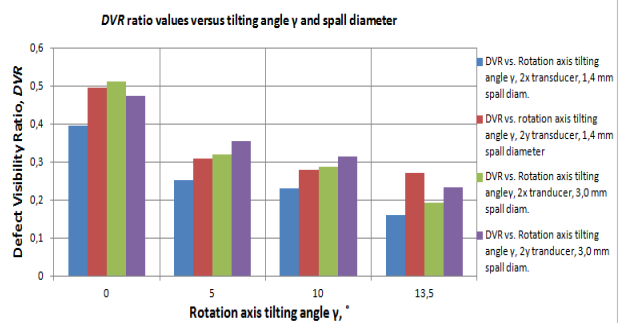


Fig. 10. DVR versus vertical axis tilt angles $\gamma = 0^0, 5^0, 10^0$ and $13,5^0$: $u_{per} = 120 \text{ g mm}$, outer rings spall diameters 1,4 mm and 3,0 mm, rotational speed $n = 3000$

In the case of vertical rotor axis $\gamma = 0^0$ and bearing small spall diameter (1,4 mm) DVR increases with increasing rotor's imbalances and slightly dependent of transducers 2X and 2Y locations (Fig.9). When the outer raceway spall diameter is 2,14 times larger (3,0 mm) the DVR decreases with increasing imbalances because the bearing's balls rotate through outer ring spall in enlarge contact area. The spall damping effect increases and BPFO vibration velocity v_{RMS_DEF} values decreases (FIG.9).

With increasing rotor's vertical axis tilting angle γ the DVR

values decrease and slightly depends on rotor's imbalance (Fig.10) and transducers locations 2X or 2Y. This factor indicates that DVR can be adopted to evaluate rotors vertical angle position in the cases of installation of new machines not only for evaluation of technical condition of vertical rotors axis position and damaged bearings.

V. Conclusions

Theoretically simulated vertical axis rotor dynamic force F_s , position angle φ can be used for evaluations not only for degradations of technical condition of bearing's elements or bearings housing, but for control of the rotors vertical axis position reference to ideal vertical axis position; it is important for industry when rotational speeds of rotors in technological machines varies at run up and coast down including resonance rotational speeds.

In the case of rotor vertical axis small tilting angle (e.g. $\gamma < 5^\circ$) the vibration velocity values measured with X and Y axis located transducers are the same order. But as tilt angle axis increased (e.g. $\gamma > 5^\circ$), the acting forces on bearings are different - vibration velocities values measured with Y transducer location is 20% higher in comparison with X transducer location.

In the case of bearing's outer raceway small spall (1,4 mm as the initial defect in first phase of degrading bearing) with increasing dynamic force F_s , the ball contact area with spall increases, and damaged bearings indications parameter DVR increases, but in the case of large spall (3,0 mm) the DVR values decreases, because the damping effect during rotation ball contact with enlarged spall on outer ring raceway increases.

The DVR parameter has been applied for vertical rotors with bearing's outer raceways defects but in future work it will be applied to study rotors dynamics with bearing's inner ring raceways artificially designed or naturally defects.

References

- [1] Tadžijevas A., Barzdaitis V., Vasylius M., Mažeika P. The Comparison of Diagnostic Features Between the Vertical and Horizontal Axis Rotors// Journal of Vibroengineering. Kaunas: Vibrotechnika. ISSN 1392-8716. Vol. 15. Issue 2 p. 1011-1019, 2013.
- [2] Tadžijevas A., Barzdaitis V., Mažeika P., Vasylius M.; Influence of Imbalance Force Angular Position to Vertical and Horizontal Rotors Rolling Bearings Defects Diagnostics// Journal of Vibroengineering. Kaunas: Vibrotechnika. ISSN 1392-8716, Vol. 16. Issue 3, p. 1475-1482, 2014.
- [3] A.Muszynska. Forward and Backward Precession of a Vertical Anisotropically Supported Rotor, Journal of Sound and Vibration, V192, n 1, p. 207-222, 1996.
- [4] Bently, D.E., Ch. T. Hatch.Fundamentals of Rotating Machinery Diagnostics, Printed in Canada, first printing. Library of Congress Control Number 2002094136, Bently Pressurized Bearing Company p.726, 2002.
- [5] Goldin, A. S. Vibration of Rotating Machines, ISBN 5-217-02927-7, UDK 621.752, BBK 22.23 G63.-Moscow: Mashinostroenie, p. 344, 2000.(in Russian).
- [6] D. Ho, R. B. Randall. Optimization of Bearing Diagnostic Techniques Using Simulated and Actual Bearing Fault Signals.Mechanical Systems and Signal Processing, 14(5), p.763-788, 2000.
- [7] Rao A., Rotordynamic Capabilities in ANSYS Mechanical. ANSYS Advantage Vol. I, Issue 2, p. 31-33, 2007.

[8] Tuncy Karacay, Nizami Akturk. Experimental diagnostics of ball bearings using statistical and spectral methods. Tribology International, Vol. 42, p. 836-843, 2009.

[9] Bently D. E., Goldman P., Yu J.J. Rolling Element Bearing Defect Detection and Diagnostics Using REBAM Probes. Orbit , p. 12-25, 2001.

[10] R. B. Randall, N. Sawalhi. Signal Processing Tools for Tracking the Size of a Spall in a Rolling Element Bearing. Proceedings of the IUTAM Symposium on Emerging Trends in Rotor Dynamics, New Delhi, India, March 23-26, 2009. Editor K. Gupta. Springer Dordrecht Heidelberg London New York, p. 429-440, 2011.